

3
P-21

Semi-Annual Progress Report

NASA Research Grant NAG-1-1072

**The Dynamics and Control of
Fluctuating Pressure Loads in the Reattachment Region
of a Supersonic Free Shear Layer**

By

A. J. Smits
Gas Dynamics Laboratory
Department of Mechanical and Aerospace Engineering
Princeton University
Princeton, N. J. 08544

NASA-Langley Research Center
Attn: Dr. W. Zuromski
Chief Scientist, Acoustics Division

C/- Dr. Jay C. Hardin
Mail Stop 461
NASA Langley Research Center
Hampton, VA 23665-5225

Covering the Period 1/1/90 through 6/30/90

(NASA-CR-184943) THE DYNAMICS AND CONTROL
OF FLUCTUATING PRESSURE LOADS IN THE
REATTACHMENT REGION OF A SUPERSONIC FREE
SHEAR LAYER Semiannual Progress Report, 1
Jan. - 30 Jun. 1990 (Princeton Univ.) 21 p G3/02

N90-27652

Unclas

0302463

Abstract

This report is the first semi-annual progress report for NASA Research Grant NAG-1-1072, administered by Dr. William E. Zorumski, and in his absence by Dr. Jay C. Hardin, of Langley Research Center.

The primary aim of this research program is to investigate the mechanisms which cause the unsteady wall-pressure fluctuations in shock wave turbulent shear layer interactions. The secondary aim is to find means to reduce the magnitude of the fluctuating pressure loads by controlling the unsteady shock motion. The particular flow proposed for study is the unsteady shock wave interaction formed in the reattachment zone of a separated supersonic flow. Similar flows are encountered in many practical situations, and they are associated with high levels of fluctuating wall pressure.

In the work performed to date, wall pressure fluctuations have been measured in the reattachment region of the supersonic free shear layer. The free shear layer was formed by the separation of a Mach 2.9 turbulent boundary layer from a backward facing step. Reattachment occurred on a 20° ramp. By adjusting the position of the ramp, the base pressure was set equal to the freestream pressure, and the free shear layer formed in the absence of a separation shock. An array of flush-mounted, miniature, high-frequency pressure transducers was used to make multichannel measurements of the fluctuating wall pressure in the vicinity of the reattachment region. Contrary to previous observations of this flow, the reattachment region was found to be highly unsteady, and the pressure fluctuations were found to be significant. The overall behavior of the wall pressure loading is similar in scale and magnitude to the unsteadiness of the wall pressure field in compression ramp flows at the same Mach number. Rayleigh scattering was used to visualize the instantaneous shock structure in the streamwise and spanwise direction. Spanwise "wrinkles" on the order of half the boundary layer thickness were observed.

These results were reported in AIAA Paper 90-1461 "Wall pressure fluctuations in the reattachment region of a supersonic free shear layer", by Z.-H. Shen, D.R. Smith, and A.J. Smits, at the AIAA 21st Fluid Dynamics, Plasma Dynamics and Lasers Conference, June 18-20, 1990, Seattle, Washington. A detailed summary is given below.

1. Introduction

The separation and reattachment of compressible turbulent flows is of significant interest in the design of high speed vehicles. Of particular interest is the highly unsteady shock motion observed near points of separation and reattachment. It has been widely shown that motion of the shock results in high amplitude pressure loads, at frequencies below 1 kHz, and these pressure loads can cause severe structural damage through fatigue. Past work has concentrated on studying the mechanisms of the shock motion near the separation point, and, although reattaching shear flows have been extensively probed^[1-7], few studies have concentrated on the flow behavior in the region of the reattachment point. The physics of shear layer reattachment, the motion of the reattachment shock, the characteristics of the wall pressure loading in the reattachment zone, and the development of the flow downstream of reattachment is still unclear.

To study these questions, it is useful to uncouple the separation process from the reattachment process: the coupling between separation and reattachment via the recirculating zone may hinder our understanding of the reattachment phenomena^[3]. The current study was designed for that purpose, that is, to examine the unsteady shock wave interaction formed in the reattachment zone of a separated supersonic flow, where the separation had occurred in the absence of a separation shock.

In the particular flow examined here, a large separated zone was formed downstream of a backward-facing step (see Fig. 1). The shear layer reattached on a 20° ramp. The position of the ramp was adjusted so that no flow expansion or lip shock wave was present at the point of separation. The upstream, freestream Mach number was 2.9, and the unit Reynolds number was $6.7 \times 10^7/\text{m}$. Measurements of the mean static pressure, and of the mass-flux fluctuations in the free shear layer, were previously made by Settles et al.^[1,2] and Hayakawa, Smits and Bogdonoff^[3]. These studies showed that the shear layer became self-similar at about 17 initial boundary layer thicknesses downstream of the lip, and that it grew at a rate typical of compressible free shear layers at this Mach number (about 1/3 the incompressible growth rate). The objective of the current experimental work was to study the fluctuating wall pressure both upstream and downstream of

the reattachment point. By examining basic statistics, including spectra and space-time correlations, some features of the unsteady reattachment and recovery processes are illustrated and discussed. It was also possible to visualize the instantaneous shock structure using Rayleigh scattering^[11], and these images shed some interesting light on the complexity of the shock-turbulence interaction.

2. Experimental procedure

All tests were made in the Princeton University 203 mm x 203 mm, high Reynolds number, blowdown, supersonic wind tunnel at a freestream Mach number of 2.92 and a unit Reynolds number of $6.7 \times 10^7/\text{m}$. The freestream turbulence level, $\langle(\rho u)'\rangle/\rho_\infty u_\infty$, was about 0.0075 [10]. Wall conditions were near adiabatic.

The test model, shown in Fig. 1, consists of a 229 mm flat plate followed by a rearward-facing step, a reattachment ramp 160 mm long, and a pair of aerodynamic fences to insure flowfield two-dimensionality. The entire model was mounted away from and parallel to the tunnel floor. The backward-facing step was 25.4 mm high. The ramp was inclined at 20 degree to the horizontal, and it was adjusted so that neither the pressure nor the flow direction changed when the boundary layer separated.

The incoming boundary layer developed on the flat plate, with transition occurring naturally within 30 mm of the plate leading edge^[1,2], so that it was representative of a fully turbulent two-dimensional self-preserving boundary layer. The boundary layer thickness δ_0 at separation was about 3.28 mm. Refs. 1 and 2 give further details of the experimental configuration.

The distance x is measured in the downstream direction along the ramp face, with the origin at the leading edge of the ramp.

2.1 Pressure Measurements

Measurements of wall pressure fluctuations were made with four Kulite miniature high frequency differential pressure transducers (Model XCQ-062-25-D). Each transducer had a 0.71 mm diameter silicon sensing diaphragm on which a fully active Wheatstone bridge was bonded atomically. The natural frequency of the transducers was 500 KHz, as reported by the manufacturer, and previous work with these transducers has shown that the upper frequency

response was limited to about 50 kHz.

The four transducers were mounted streamwise, 5.05 mm (0.2 inches) apart, and offset from the centerline by 2.54 mm. The transducers were adjusted to be flush to the surface less than $0.002 \delta_0$, to minimize any interference effects on the flow^[13].

Each transducer - A/D converter link was regularly calibrated statically at the operating temperature. The calibrations were linear and the slope remained constant within 1% throughout the experiments. Tests in a shock tube have shown that transducer of this type have dynamic calibrations only a few percent lower than those obtained statically^[14].

Simultaneous signals from each transducer were amplified by a two-stage amplifier (-3dB point at 120 KHz) at gains of 500 or 1000. The signals were then band-pass filtered between 50 Hz and 80 KHz by Ithaco 4213 analog filters (fourth-order Butterworth). The sampling rate was 500 KHz. The analog signals were further amplified with gains between 0.5 and 0.2, and then digitized with a CAMAC (Computer Aided Measurement And Control) system linked to a VAX 750. The data were obtained in files of 4 records, each record consisting of 98K sample points. Data processing included calculation of power spectra, cross-spectra, coherence, autocorrelation and space-time correlations, as well as the probability distribution functions.

2.2 Rayleigh Scattering

Rayleigh scattering is the elastic scattering of photons by particles much smaller than the wavelength of the incoming light. The images presented here were made possible by using a high-power, Nd:YAG laser operating in the far-ultraviolet in conjunction with a high-sensitivity, far-ultraviolet camera. By focusing the laser into a thin sheet of light and passing it through the wind tunnel, cross-sectional images of the air density can be recorded by direct Rayleigh scattering. For the pictures shown here, the illumination is with a Quantel International YG661 laser operating in the vicinity of .266 microns with a pulse duration of 4 nsec, so the cross-sectional image is frozen in time. The tunnel and the model were fitted with UV transmitting quartz windows so that the laser sheet could be passed through the flow field. The high-sensitivity camera observed the scattering at 90° and images could be recorded up to the laser pulsing rate of 10 Hz.

The presence of water in the air can have a strong effect on the interpretation of these images, even for extremely low water concentrations (parts per million). Upstream of the nozzle, where it is in the form of water vapor, its Rayleigh cross section is small. However, as the flow expands through the nozzle, the water molecules can agglomerate into very small ice clusters of the order of 30 nanometers in diameter¹⁵. When they are present in sufficient numbers, these small particles dominate the Rayleigh signal. Quantitatively, therefore, the images obtained in air give the density of these ice clusters rather than the density of air. Now, it appears that the ice crystal density is nearly proportional to the local air density, except in regions where the temperature rises to the point where the ice returns to the vapor phase. There are two main consequences: we lose some resolution near the wall, where the frictional heating increases the temperature, and strong shocks become visible as lines separating bright zones (low temperature) from dark zones (high temperature), whereas weak shocks are seen as lines separating bright zones from even brighter zones.

Current work is directed towards the quantitative interpretation of these images, which means in effect determining the connection between the local image intensity which is related to the local density of the ice clusters, and the density of the air at that point. Even qualitatively, however, the Rayleigh images provide valuable information on the interaction between the turbulence and the reattachment shock, as well as providing some interesting images of the turbulence structure of the incoming shear layer.

3. Wall Pressure Results

The average reattachment line was found by using the kerosine-graphite technique on the surface of the ramp. Reattachment was located approximately 2.65 ± 0.05 inches away from the edge of the ramp^[10]. The previous work by Settles et al.^[2] were obtained under the same conditions as those of the present tests. The overall mean flow field, and the mean static pressure distribution is shown in Fig. 2.

Fig. 3 shows the normalized RMS wall pressure for the transducers located upstream and downstream of the mean reattachment point. In Fig. 3a, it is seen that near the reattachment point, the normalized pressure fluctuation level, σ_{pw}/p_w , has a maximum value of about 9%, where σ_{pw} and p_w

are the RMS value of wall pressure fluctuation and local mean static pressure, respectively. It is worth noting that the incoming boundary layer values were about 1% [10]. These pressure fluctuation magnitudes are similar to those reported by Dolling et al. [5] for a 20° compression ramp, where σ_{pw}/p_w reached a maximum of about 9 percent near the mean reattachment point. However, under the present conditions, the maximum pressure fluctuation occurs about $2\delta_0$ downstream of the mean reattachment point, where δ_0 is the boundary layer thickness at the reattachment point (0.6" or 15 mm). Furthermore, downstream, the fluctuation level drops gradually, although the level remains at a value greater than that of the incoming flow, even at the furthest downstream measuring station $5\delta_0$ downstream of the reattachment point.

For comparison, the absolute level of the RMS wall pressure, normalized by the upstream mean static pressure p_{w0} , σ_{pw}/p_{w0} , is shown in Fig. 3b. This increases sharply to a maximum of 30%, at a point δ_0 downstream of the reattachment point, then decreases slowly (with considerable scatter in the data).

The increase in the RMS pressure fluctuation level near the reattachment point is similar to the increase observed in the maximum level of the RMS mass-flux fluctuations [2-3] (see Fig. 4). As indicated by Hayakawa et al. [3], the intensity of the mass-flux fluctuations in the free shear layer increases slowly with downstream distance. Then the maximum turbulence intensity rises rapidly as the shear layer approaches the ramp, and at reattachment it reaches a level of almost 40%. Downstream of this point, the intensity continues to rise before reaching a maximum at about $3\delta_0$ downstream of reattachment.

The energy spectra of the pressure fluctuations at selected positions are shown in Fig. 5a, b, c, d and e, respectively. The energy spectra are plotted as $G(f) \cdot f \sim \log(f)$, where f is the frequency. Therefore, the area under the curve delimited by two frequencies f_1 and f_2 denotes the energy content within that frequency range. At $x = 2.05$ " (52 mm), which is located upstream of the reattachment point, the energy spectrum is centered around 12 KHz (Fig. 5a). Note that the incoming typical eddy frequency, U_∞/δ_0 , is 170 KHz, where U_∞ is the freestream velocity. At $x = 2.75$ " (70 mm), just downstream of the reattachment point, the fluctuation energy increases

sharply but the frequency content of the spectrum does not change very much (Fig. 5b). Further downstream at $x = 2.95$ " (75 mm), the fluctuation energy continues to increase quickly (and shifts towards higher frequencies) while the amplitudes of the lower frequencies decrease, which seems to indicate a breakdown of large scale structures to smaller scales. Further downstream, Fig. 5d shows that the frequency content and the amplitude of the energy appear to begin a recovery process, but even near the end of the ramp (Fig. 5e) neither the frequency content nor the amplitude of the energy is very similar to that of an undisturbed boundary layer at about the same Reynolds number.

The probability density distributions of the wall pressure fluctuations are shown in Fig. 6 a, b, c, d, e and f. The solid lines are the equivalent Gaussian distributions. Upstream of the reattachment point, as shown Fig. 6b, there was a significant positive skewness coefficient, α_3 . This indicates that there exist large scale structures which are lagging behind the mean flow⁴. The intermittent nature of the instantaneous wall pressure in the reattachment and redevelopment regions gives rise to a bimodal pdf at $x = 2.75$ ". Downstream from the mean reattachment point at $x = 2.65$ ", a new boundary layer begins to develop, and α_3 shifts to about 0. On the other hand, the flatness coefficient α_4 reaches a minimum near reattachment (Fig. 6c), then quickly recovers to about 3.0 and appears again like a Gaussian distribution.

Figs. 7 and 8 show the space-time correlations between two signals with three different longitudinal separation distances: 0.2", 0.4", and 0.6" (5.1 mm, 10.2 mm, and 15.2 mm, or $0.33\delta_0$, $0.68\delta_0$, and $1.02\delta_0$), respectively. The position of the first transducer (located at the most upstream point) is given in the figures. At $x = 2.5$ ", the maximum cross-correlation levels are considerably lower than that in an undisturbed boundary layer at a similar Reynolds number (see Fig. 9). At positions downstream of reattachment, however, these values increase to about 0.7, and the correlations appear to decay at a rate similar to that observed in a fully developed boundary layer (Fig. 9).

4. Rayleigh Scattering Results

A preliminary visualization study using the Rayleigh technique yielded

some interesting results. The image given in Fig. 10 shows the view in a streamwise plane near reattachment, indicating the apparent shock splitting, which seems to extend considerably upstream of the mean reattachment point. No two images are alike, showing that the strong pressure fluctuations observed on the ramp indicate a high degree of unsteady shock motion.

When the plane of the light sheet is oriented parallel to the freestream direction, the image gives an instantaneous plan view of the large scale organization of the shear layer. Some planviews give a strong indication that a spanwise, and a streamwise structure exists, in accordance with previous subsonic observations at low Reynolds number. Near the ramp (Fig. 11), the streamwise organization is particularly evident, suggesting the presence of Taylor-Gortler-like vortices near reattachment, as has been speculated in the past (Selig et al.^[10]). When the plane of light is tilted so that it makes an angle of about 20° with the plane of the ramp, a most remarkable wrinkling of the reattachment shock is made visible (Fig. 12). This visualization of the instantaneous wrinkling of the shock sheet is the first ever obtained.

In future work, we intend to couple the Rayleigh flow visualizations with the wall-pressure measurements, so that we can determine more directly the coupling between the incoming turbulent motions and the wall pressure.

5. Summary and Conclusion

The present experiment investigated the nature of fluctuating wall pressure in the reattachment and redevelopment region of a two-dimensional supersonic free shear layer. RMS pressure levels and space-time cross-correlation measurements were obtained, as well as some preliminary images of the instantaneous shock structure.

In the pressure fluctuation data, the most remarkable feature observed was the dramatic increase in large amplitude pressure fluctuation near the reattachment point, which reached a maximum of about 11% of the local mean pressure. The pressure fluctuations fall off gradually in the redeveloping boundary layer downstream. The results also show that the flow on the ramp is divided into two regions, a reattachment and a redevelopment region. Near reattachment, pressure fluctuations greatly increase, and large scale structures breakdown into smaller scales. Downstream of reattachment, the

fluctuating properties gradually decline and the boundary layer recovers its structure.

The Rayleigh scattering images showed that the instantaneous shock structure in the reattachment zone is very complex: there is streamwise shock splitting, and spanwise shock wrinkling, so that there can exist "cells" enclosed by shock sheets. The connection between the shock structure, the incoming turbulence, and the wall pressure field is yet to be made, and this will be the subject of future work.

6. Future Work

In the first year, it was proposed to extend our investigation of the fluctuating wall pressure field to study the scale of the unsteady shock motion, and the corresponding turbulence scales, using multiple arrays of miniature Kulite pressure transducers to give data for analysis by conditional sampling and correlation techniques. At the same time, the model was to be modified to accept a quartz window, and we would make the first direct visualizations of the instantaneous density field using Rayleigh scattering. At this time, the pressure measurements are complete, and the preliminary Rayleigh images have been obtained. In the remaining period of the first year, we intend to complete the analysis of the pressure data, and the final results will be incorporated with the work reported in AIAA Paper 90-1461 "Wall pressure fluctuations in the reattachment region of a supersonic free shear layer", by Z.-H. Shen, D.R. Smith, and A.J. Smits, at the AIAA 21st Fluid Dynamics, Plasma Dynamics and Lasers Conference, June 18-20, 1990, Seattle, Washington, and submitted to the AIAA Journal.

In the second year, we intend to couple the Rayleigh flow visualizations with the wall-pressure measurements, so that we can determine directly the coupling between the incoming turbulent motions and the wall pressure. These measurements will be the first of their kind, and they are expected to give a totally new insight in the mechanisms which drive the flow unsteadiness. The technique for acquiring Rayleigh images and pressure signals simultaneously is currently being tested for use in the reattaching shear layer geometry. In concurrent work, we will analyze the Rayleigh scattering images to obtain quantitative data on the density field, such as rms intensity levels, probability density distributions, and space correlations.

Using these quantitative techniques, we hope to establish the statistical properties of the average large-scale motion interacting with the shock wave.

In the third year, we will begin the application of control methods in an attempt to reduce the level of the fluctuating pressure loads. The particular control methods chosen will depend largely on the results obtained in the first two years. If a strong link is established between the incoming turbulence and the wall pressure fluctuations, we intend to modify the incoming shear layer in an attempt to interfere destructively with this coupling. One way to do this may be blowing upstream of the point of separation, or blowing into the unsteady recirculation zone. Alternatively, piezzo-electric actuators, of the type used in subsonic shear layers by Professor A. Glezer of the University of Arizona, placed across the span of the upstream boundary layer may be used to enhance the three-dimensional character of the incoming motions, and thereby reduce the intensity of the flapping motion.

References

1. Baca, B. K. M., Sc. Dissertation, Princeton University, Princeton, N.J., 1981.
2. Settles, G. S., Baca, B. K., Williams, D. R., and Bogdonoff, S. M., "A Study of Reattachment of a Free Shear Layer in Compressible Turbulent Flow," AIAA Journal, Vol. 20, pp. 60- 67, 1982.
3. Hayakawa, K., Smits, A. J. and Bogdonoff, S. M., "Turbulence Measurements in a Compressible Reattaching Shear Layer", AIAA Journal, Vol. 22, pp. 889-895, 1984.
4. Samimy, M. and Abu-Hijleh, B. A./K., "Structure of a Reattaching Supersonic Shear layer", 88-3615, 1988.
5. Dolling, D. S. and Murphy, M. T., "Unsteadiness of the Separation Shock Wave Structure in a Supersonic Compression Ramp Flowfield", AIAA J., 21, 1628-1634, 1983.
6. Dolling, D. S. and C.T., Or, "Unsteadiness of the Shock Wave Structure in Attached and Separated Compression Ramp Flowfields", Exp. in Fluids, 3, 24-32, 1985.
7. Dolling, D. S. and Brusniak, L., "Separation Shock Motion in Fin, Cylinder and Compression Ramp-Induced Turbulent Interactions", AIAA Paper 87-1368, 1987.
8. Muck, K., Dussauge, J.-P. and Bogdonoff, S. M., "Structure of the Wall Pressure Fluctuations in a Shock-Induced Separation Turbulent Flow", AIAA 85-85-0179, Jan. 1987.
9. Muck, K. C., Andreopoulos, J. and Dussauge, J-P., "Unsteady Nature of Shock-Wave/Turbulent Boundary Layer Interaction", AIAA Journal, Vol. 26, pp. 179-187, 1988.
10. Selig, M. S., Andreopoulos, J., Muck, K.C., Dussauge, J.-P. and Smits, A. J., "Turbulence Structure in a Shock-Wave/Turbulent Boundary Layer Interaction", AIAA Journal, Vol. 27, pp. 862-869, 1989.
11. Smith, M.W., Smits, A.J. and Miles, R.B. Optics Letters, 14: 916-918, 1989.
12. Spina, E. and Smits, A. J., "Organized structures in a compressible, turbulent boundary layer", JFM, Vol. 182, pp. 85-109, 1987.
13. Hanley, R. D., "Effects of Transducers Flushness on Fluctuating Surface Pressure Measurements", AIAA Paper 75-534, 1975.
14. Chyu, W. J. and Hanly, R. D., "Power and Cross Spectra and Space-Time Correlations of Surface Fluctuating Pressures at Mach Numbers Between 1.6 and 2.5", NASA TN-D-5440, 1969. Also AIAA paper 68-77.

15. Wegener, P. P. and Stein, G. D. 12th Intern. Symp. on Combustion, 1183-1191, 1968.

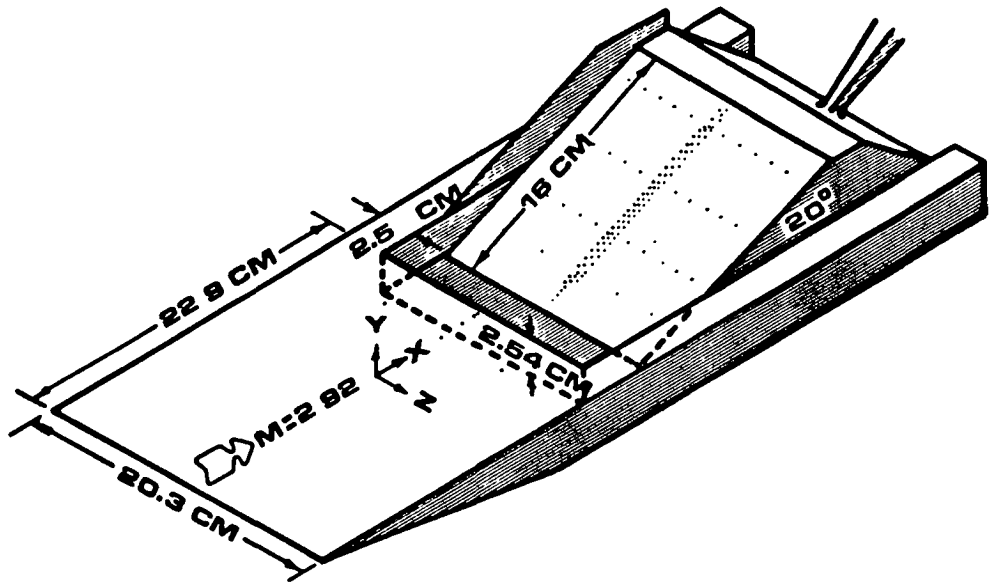


Fig 1. Geometry for the formation of a free shear layer and its subsequent attachment on a 20° ramp (from Settles et al.²).

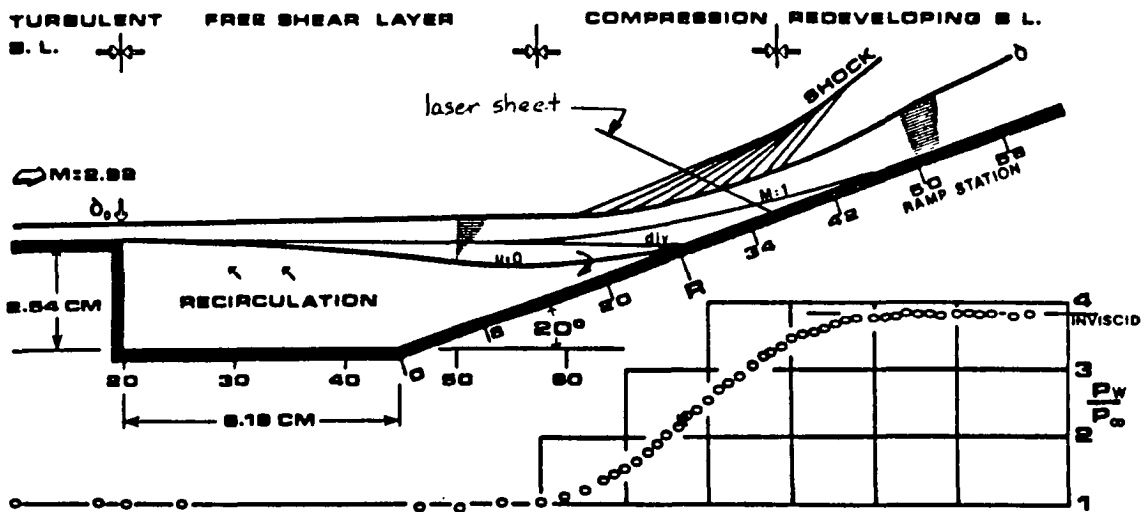


Fig. 2. Flowfield showing test model and surface static pressure distribution (from Settles et al.²).

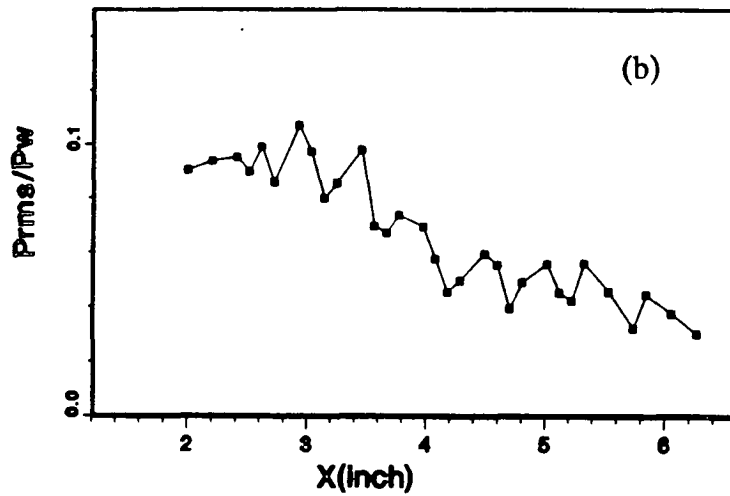
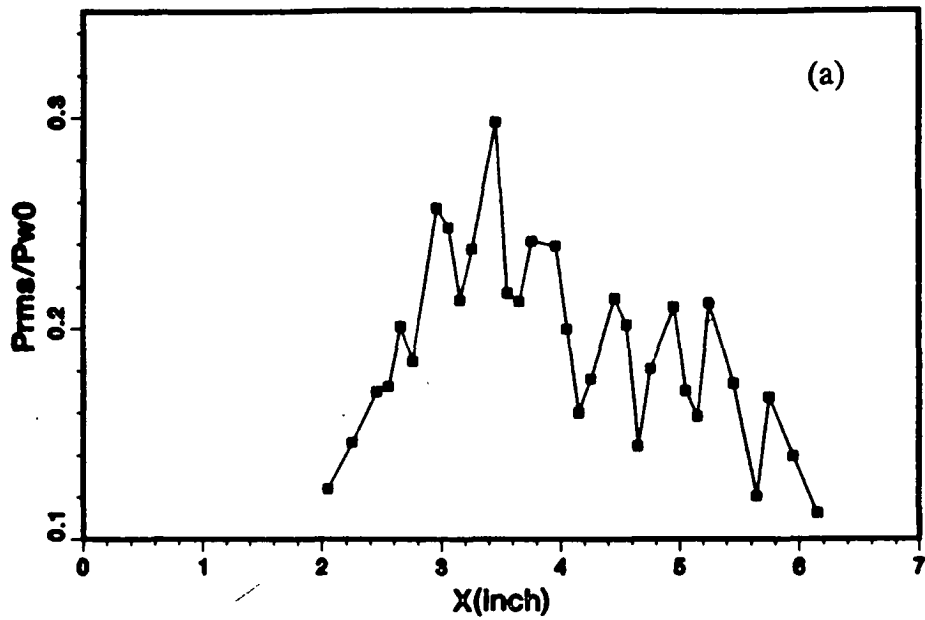


Fig. 3. RMS intensity of the wall pressure fluctuations in the reattachment zone: (a) σ_{pw}/P_w ; (b) σ_{pw}/P_{w0} .

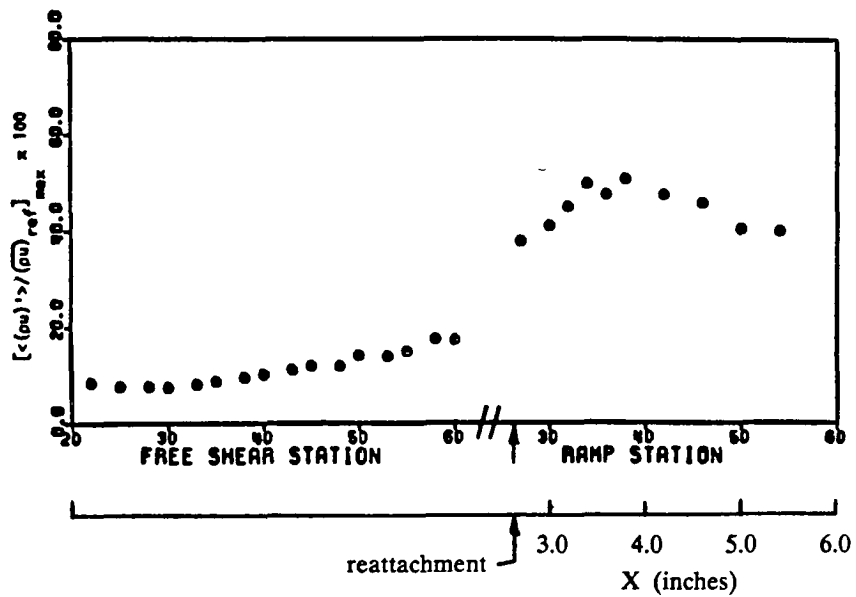


Fig. 4. Maximum level of mass-flux fluctuations in free shear layer and developing boundary layer on ramp face. Reattachment occurs at $x = 2.65$ ".

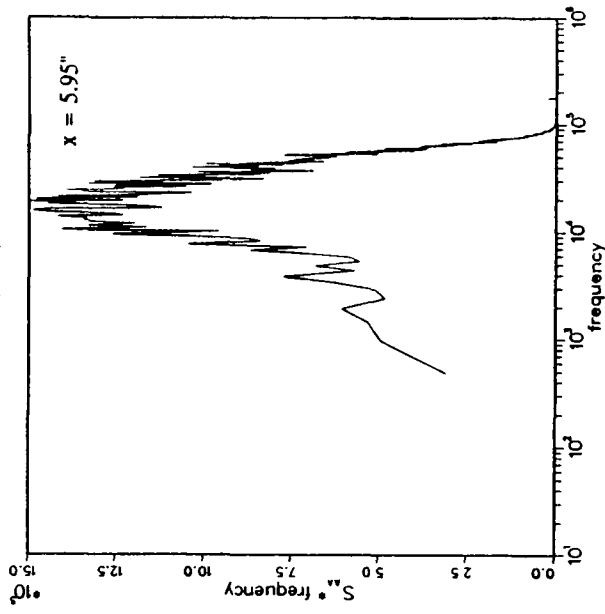
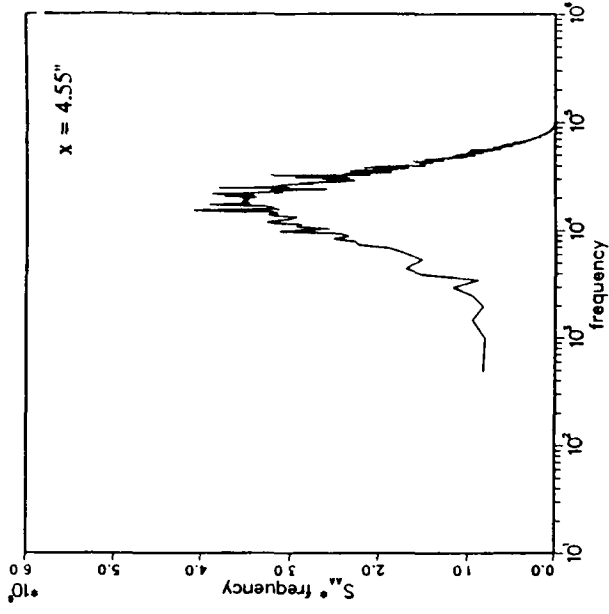
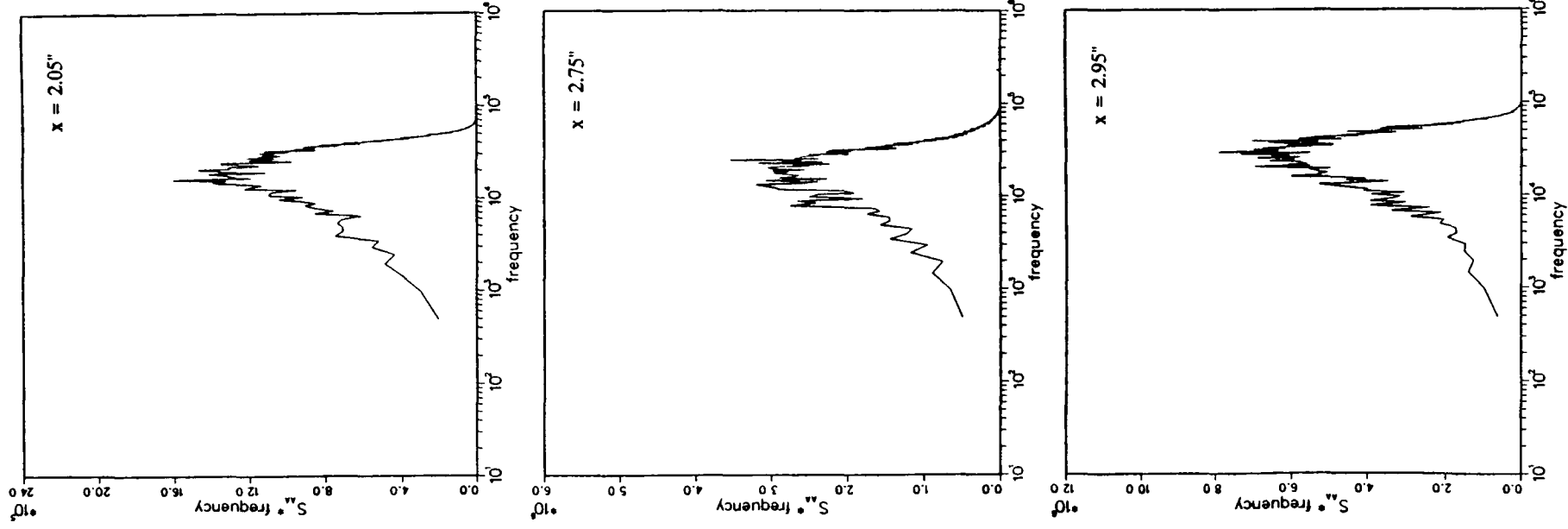


Fig. 5. Energy spectra of the pressure fluctuations on the ramp face: (a) $x = 2.05''$, (b) $x = 2.75''$; (c) $x = 2.95''$, (d) $x = 4.55''$; (e) $x = 5.95''$.

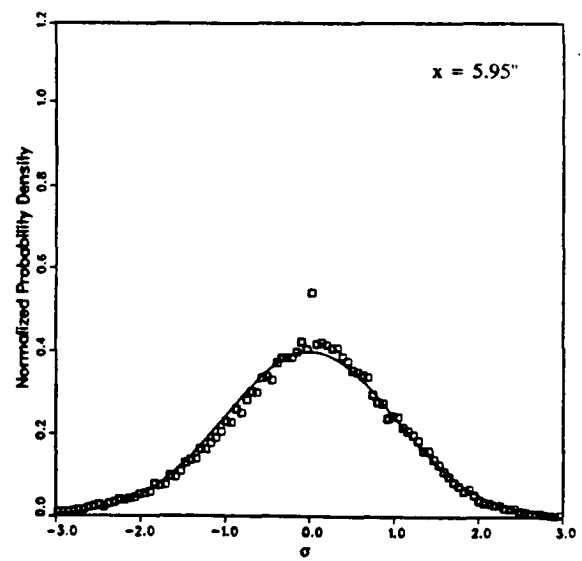
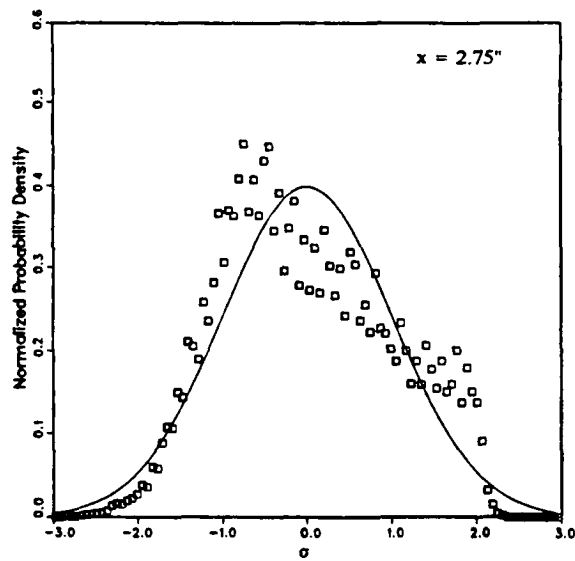
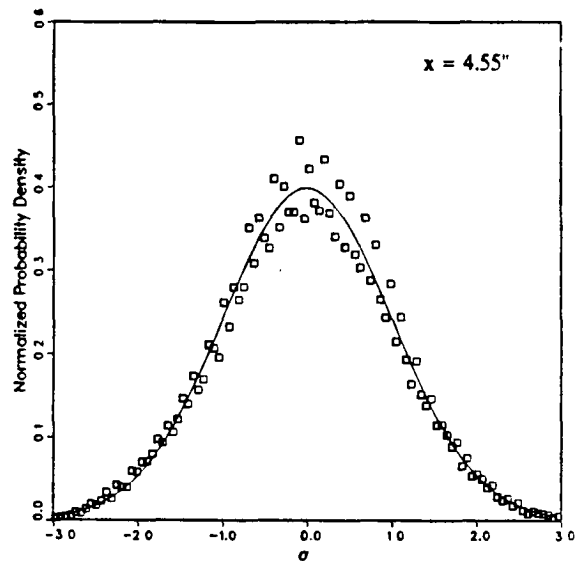
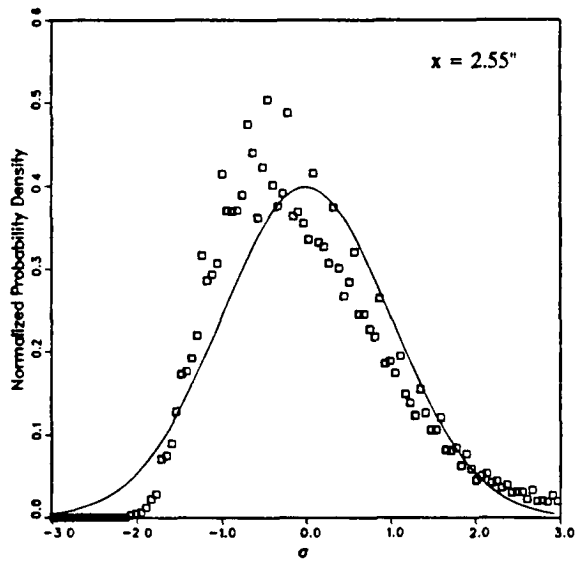
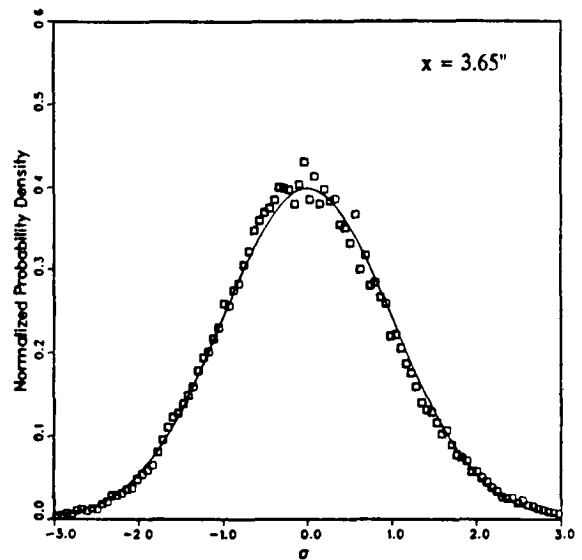
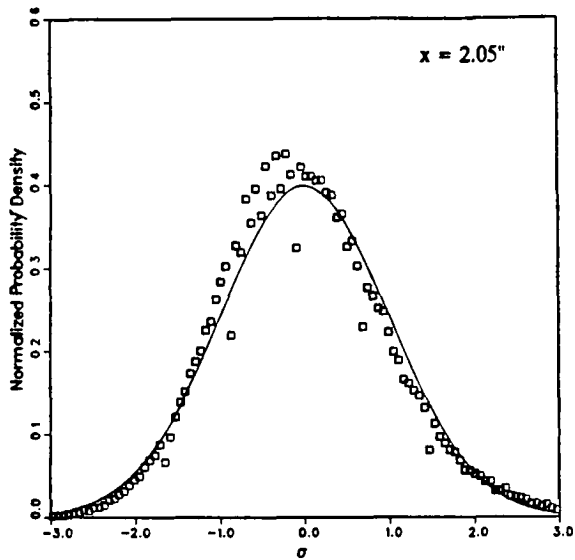


Fig. 6. Probability density distributions of the wall pressure on the ramp face: (a) $x = 2.05''$; (b) $x = 2.55''$; (c) $x = 2.75''$; (d) $x = 3.65''$; (e) $x = 4.55''$; (f) $x = 5.95''$.

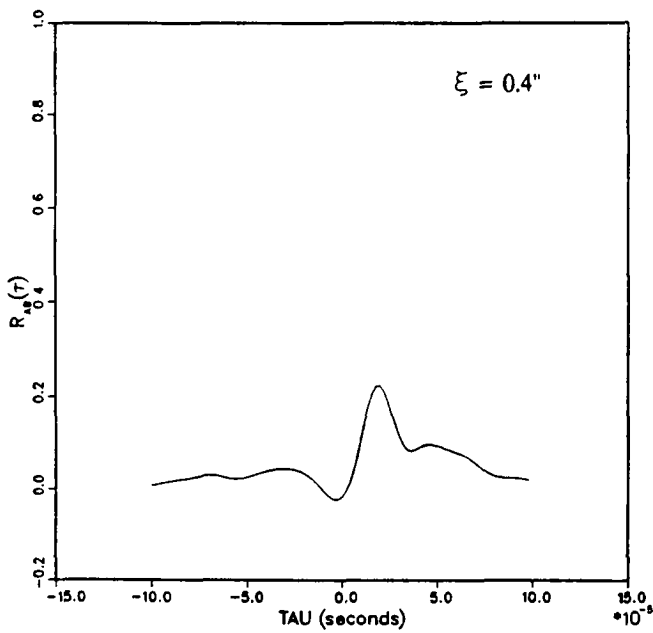
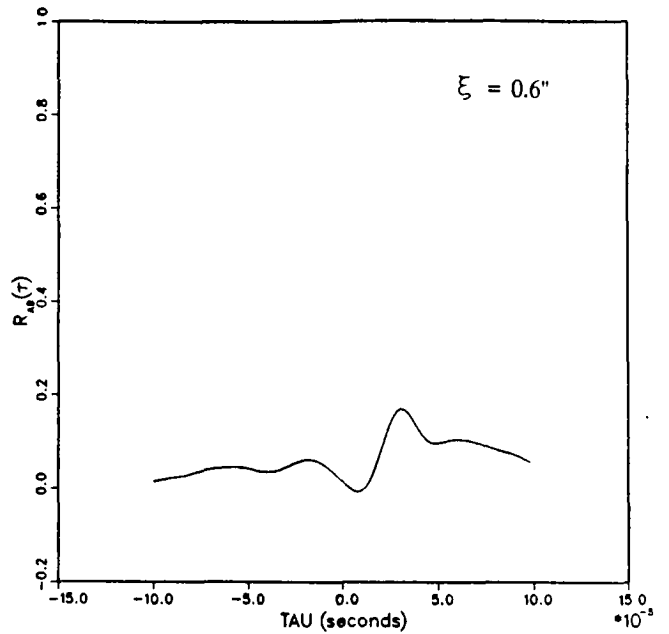
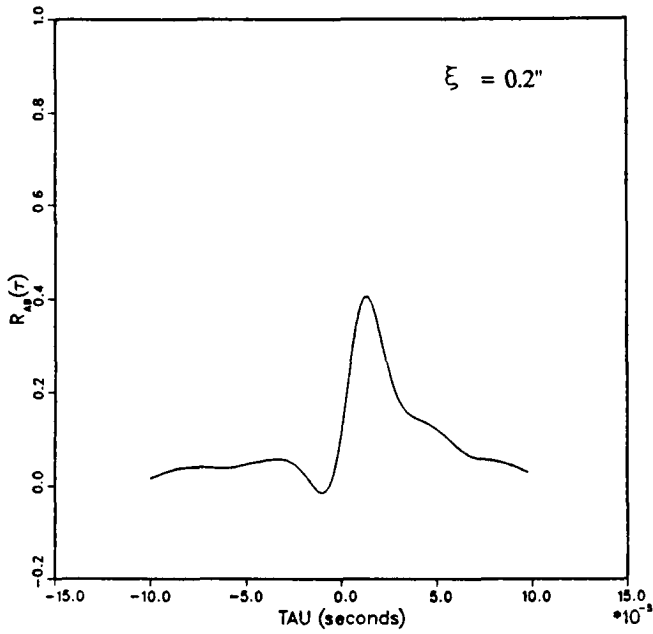


Fig. 7. Space-time correlations of the wall pressure on the ramp face at $x_1 = 2.5$ ": (a) $\xi = 0.2$ "; (b) $\xi = 0.4$ "; (c) $\xi = 0.6$ ".

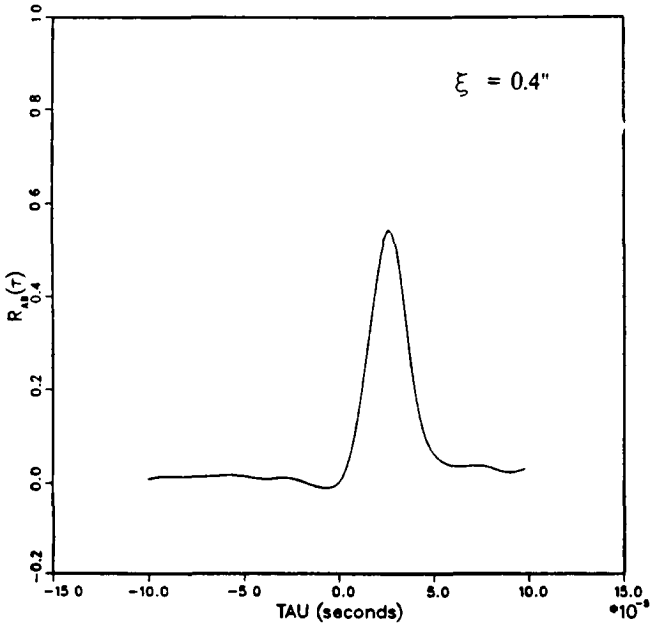
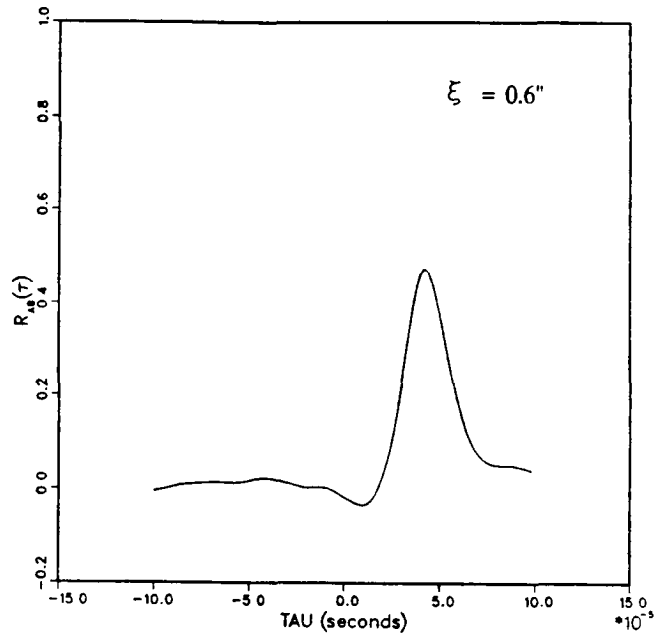
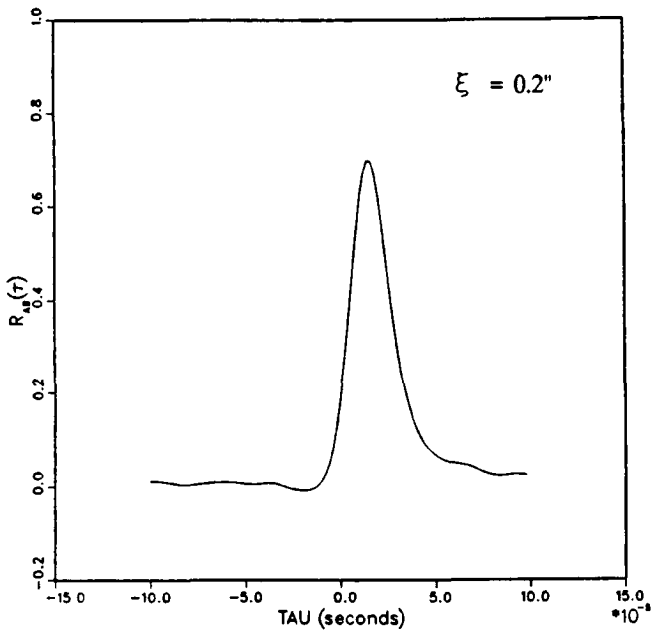


Fig. 8. Space-time correlations of the wall pressure on the ramp face at $x_1 = 4.0''$: (a) $\xi = 0.2''$; (b) $\xi = 0.4''$; (c) $\xi = 0.6''$.

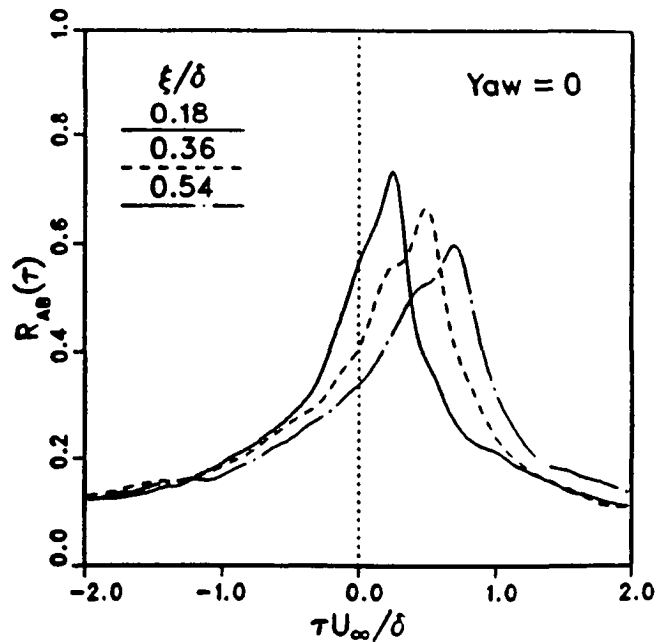


Fig. 9. Space-time correlations of the wall pressure in an undisturbed zero pressure gradient boundary layer (from Spina and Smits¹²).

ORIGINAL PAGE
BLACK AND WHITE PHOTOGRAPH

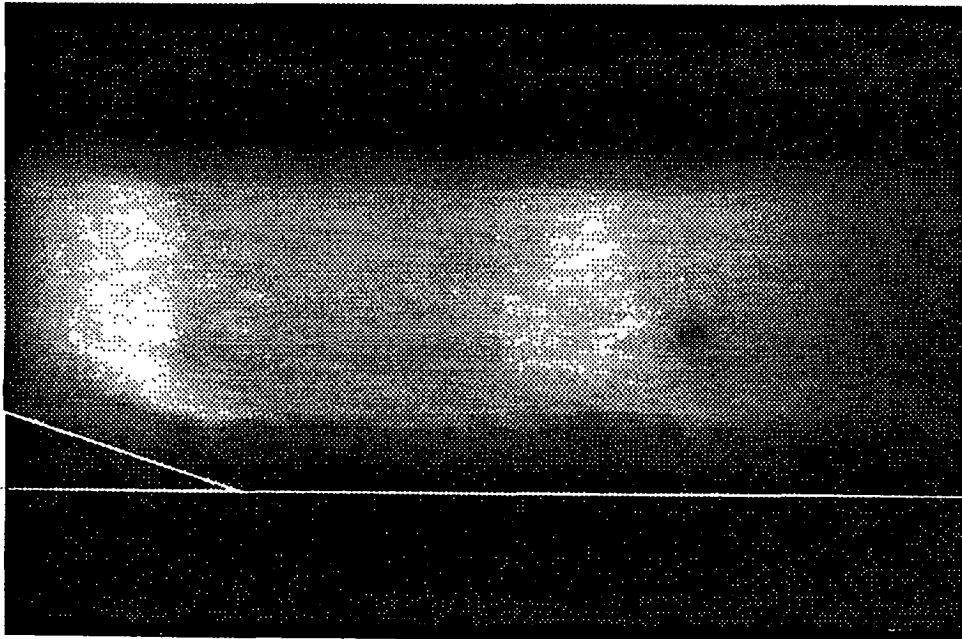
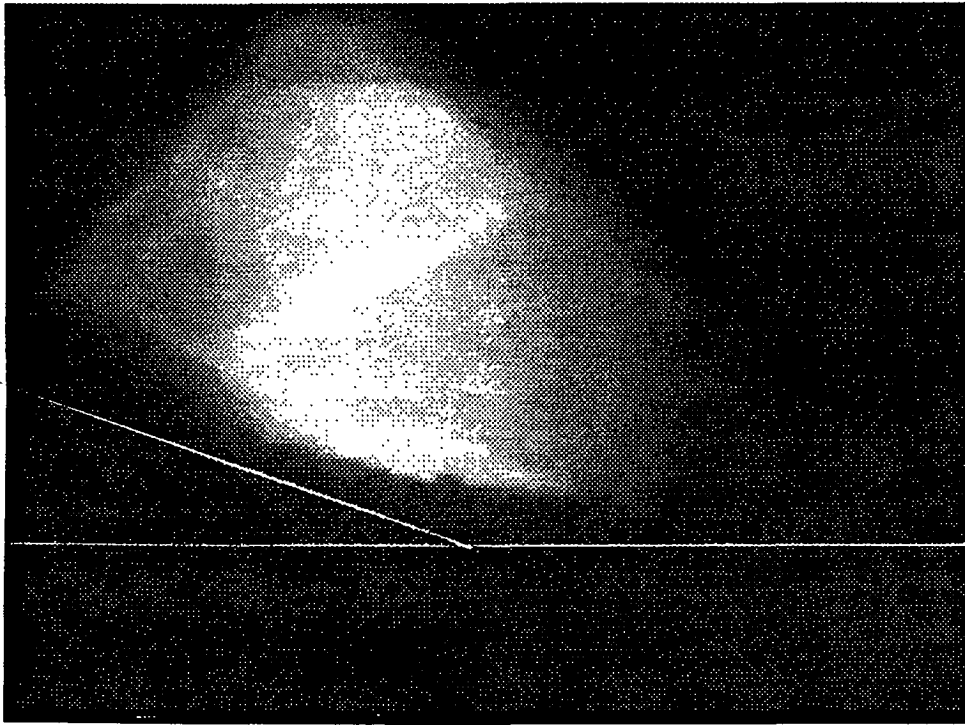


Fig. 10. Streamwise image of a reattaching free shear layer in an air flow. Flow is from right to left. The complicated shock structure near reattachment is clearly evident.

ORIGINAL PAGE
BLACK AND WHITE PHOTOGRAPH

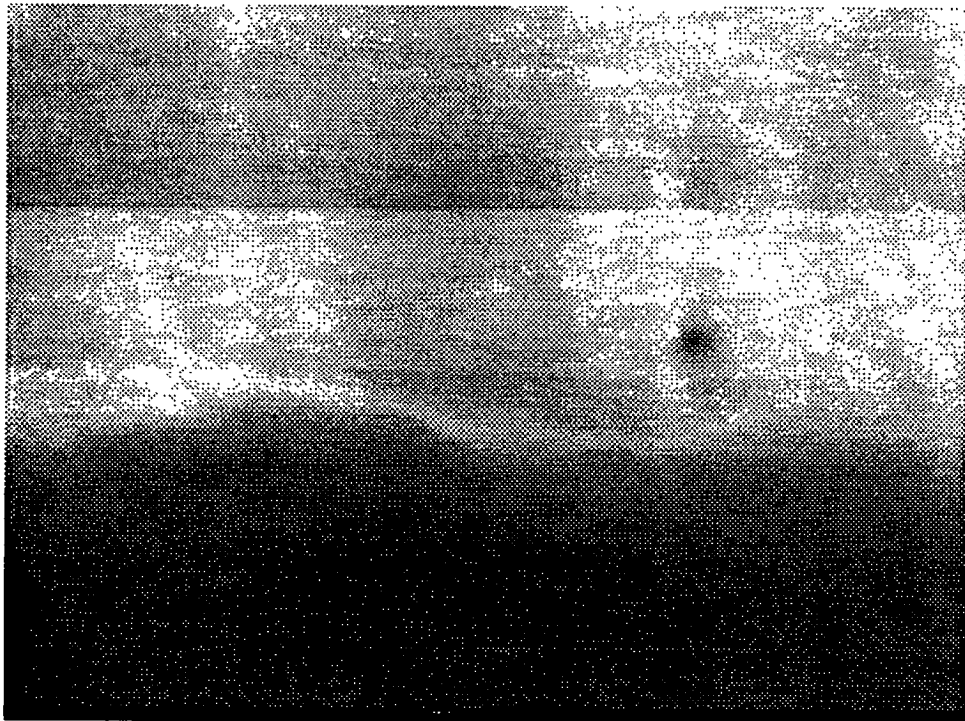
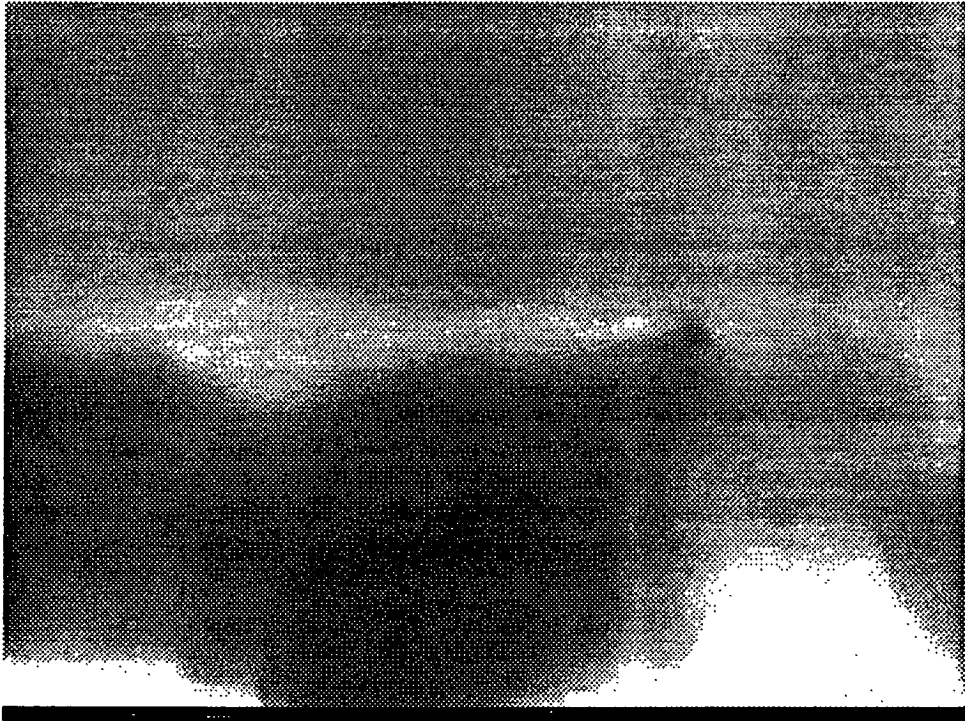


Fig. 11. Image of the attachment region of a freeshear layer on a 20° ramp in an air flow. The laser sheet orientation is shown in Figure 2. Flow is from top to bottom of the picture. Shocks show up as regions where the brightness increases (this is true as long as the temperature rise is relatively small). These images indicate that more than one shock is present in the attachment region, and that they are strongly wrinkled by the incoming turbulence.